Journal of Pharmaceutical Analysis 10 (2020) 560–570

Contents lists available at ScienceDirect

Journal of Pharmaceutical Analysis

journal homepage: www.elsevier.com/locate/jpa

Original article

# Vancomycin pretreatment attenuates acetaminophen-induced liver injury through 2-hydroxybutyric acid

Ningning Zheng [a], Yu Gu [a], Ying Hong [a], Lili Sheng [a], Linlin Chen [a], Feng Zhang [a], Jie Hou [b], Weidong Zhang [a, c], Zean Zhang [d], Wei Jia [e, f, **], Houkai Li [a, *]

[a] Institute of Interdisciplinary Integrative Medicine Research, Shanghai University of Traditional Chinese Medicine, Shanghai, 201203, China
[b] College of Basic Medical Sciences, Dalian Medical University, Dalian, 116044, China
[c] School of Pharmacy, Second Military Medical University, Shanghai, 200433, China
[d] Center for Drug Safety Evaluation and Research, Shanghai University of Traditional Chinese Medicine, Shanghai, 201203, China
[e] University of Hawaii Cancer Center, Honolulu, HI, 96813, USA
[f] Shanghai Key Laboratory of Diabetes Mellitus and Center for Translational Medicine, Shanghai Jiao Tong University Affiliated Sixth People's Hospital, Shanghai, 200233, China

ARTICLE INFO

*Article history:*
Received 9 July 2019
Received in revised form
11 October 2019
Accepted 5 November 2019
Available online 6 November 2019

*Keywords:*
revealed
Liver injury
Gut microbiota
Acetaminophen
Vancomycin
2-Hydroxybutyric acid

ABSTRACT

Liver injury caused by acetaminophen (AP) overdose is a leading public health problem. Although AP-induced liver injury is well recognized as the formation of N-acetyl-p-benzoquinone (NAPQI), a toxic metabolite of AP, resulting in cell damage, emerging evidence indicates that AP-induced liver injury is also associated with gut microbiota. However, the gut microbiota-involved mechanism remains largely unknown. In our study, we found that vancomycin (Vac) pretreatment (100 mg/kg, twice a day for 4 days) attenuated AP-induced liver injury, altered the composition of gut microbiota, and changed serum metabolic profile. Moreover, we identified Vac pretreatment elevated cecum and serum 2-hydroxybutyric acid (2-HB), which ameliorated AP-induced cell damage and liver injury in mice by reducing AP bioavailability and elevating GSH levels. Our current results revealed the novel role of 2-HB in protecting AP-induced liver injury and add new evidence for gut microbiota in affecting AP toxicity.


## 1. Introduction

Acetaminophen (AP) is a widely used over-the-counter medication for relief of pain and fever. However, liver damage caused by AP overdose is a leading public health problem. AP-induced hepatotoxicity accounts for 46% of all cases of acute liver failure in the United States [1] and 40%–70% of all cases in the Great Britain and Europe [2]. About 85% of AP undergoes phase II conjugation to sulfated and glucuronidated metabolism in the liver, and 10% of AP undergoes phase I oxidation to N-acetyl-p-benzoquinone (NAPQI), which is catalyzed by CYP2E1, CYP1A2, and CYP3A4 and normally conjugated with glutathione (GSH) to nontoxic metabolites. Overdose of AP increases NAPQI production resulting in depletion of GSH, as well as binding with cellular proteins leading to cell injury [3–5].

Gut microbiota usually modulates the oral drug bioavailability or half-life by altering the capacity of drug-metabolizing enzymes or expression of genes involved in drug metabolism in host tissues [6]. Clayton et al. [7] have observed that individuals with a high level of pre-dose urinary p-cresol, a microbial metabolite, show low post-dose urinary ratios of sulfated AP to glucuronic AP, suggesting that gut microbiota might affect the metabolism of AP. Moreover, Lee et al. have evaluated the effects of gut microbiota on AP metabolism in antibiotic-treated rats. They find antibiotic-treated rats have a higher level of AP glutathione conjugates in blood than untreated rats, suggesting the impacts of gut microbiota on AP metabolism [8]. Moreover, Gong et al. [9] have demonstrated that AP-induced rhythmic variation in hepatotoxicity is at least partially due to the production of gut microbial metabolite, 1-phenyl-1,2-propanedione, which depletes hepatic GSH levels. Such evidence suggests that microbial metabolites also play important role in affecting AP-induced hepatotoxicity. However, the microbiota-

Peer review under responsibility of Xi'an Jiaotong University.
* Corresponding author.
** Corresponding author. University of Hawaii Cancer Center, Honolulu, HI, 96813, USA.
*E-mail addresses:* wjia@cc.hawaii.edu (W. Jia), houkai1976@126.com (H. Li).

https://doi.org/10.1016/j.jpha.2019.11.003

related mechanism remains largely unexplored due to the extremely complex relationship between gut microbiota and the host.

In our present study, we observed that vancomycin (Vac) pretreatment attenuated AP-induced hepatotoxicity, as well as the alteration of gut microbiota composition, indicating the microbial impacts on AP-induced hepatotoxicity. Furthermore, untargeted and targeted metabolomics revealed that Vac pretreatment increased serum levels of 2-hydroxybutyric acid (2-HB), which attenuated AP-induced hepatotoxicity both in vitro and in vivo.

## 2. Materials and methods

### 2.1. Animals, cell lines and reagents

Male SD and Wistar rats (160–180 g) and C57 mice (18–22 g) were purchased from Shanghai SLAC Laboratory Animal Company and housed at constant temperature (24 ± 2 °C) with a 12 h light-dark cycle. BRL3A (ATCC number: CRL-1442) and AML12 (ATCC number: CRL-2254) cells were purchased from ATCC (Manassas, MA, USA). Vac was purchased from Lilly Company (USA). AP, 2-HB, phenacetin were purchased from Sigma-Aldrich (St. Louis, MO, USA). Sodium (±)-2-hydroxybutyrate-2,3,3-d3 (d3-2-HB) was purchased from C/D/N Isotopes Inc (Canada). ALT, AST kits were purchased from Nanjing Jiancheng Bioengineering Institute (China). GSH & GSSG and CCK-8 kits were purchased from Beyotime Biotechnology (China). Gut bacterial DNA extraction kit was purchased from QIAGEN Company (Germany). TRIzol reagent, reverse transcript enzyme and SYBR Green master mix were purchased from Invitrogen (Carlsbad, CA). CYP2E1 (Cat: ab28146, Lot:GR324351-11), CYP3A4 (Cat: ab3527, Lot: GR3210692-3), NQO-1 (Cat: ab2346, Lot: GR3550-44) primary antibodies were purchased from Abcam (USA). Collagenase type I (Cat: LS004196) was purchased from Washington Biochemical Corporation. Percoll (Cat: P1644) was purchased from Sigma-Aldrich.

### 2.2. Animal experiments and sample collection

The animal experiments were conducted under the Guidelines for Animal Experiment of Shanghai University of Traditional Chinese Medicine and the protocol was approved by the Institutional Animal Ethics Committee. First, to distinguish the gut microbial impacts on AP-induced acute liver injury, male SD rats were divided into three groups as follows: Con group ($n = 6$), AP (i.g) group ($n = 14$) and AP (i.p) group ($n = 8$). After overnight fasting, the rats were administered with single-dose of AP either orally (2.0 g/kg) or intraperitoneal injection (1.0 g/kg) respectively, and sacrificed 24 h after AP administration. In the second animal experiment, SD rats were divided into four groups as follows: Con group ($n = 6$), Vac group ($n = 6$), AP group ($n = 29$) and Vac_AP group ($n = 21$). Vac and Vac_AP groups were orally given Vac (200 mg/kg/d) [10] for consecutive 4 days prior to the administration of a single dose of AP (2.0 g/kg). After 24 h, all rats were anesthetized with 2% pentobarbital sodium and samples were collected and stored at −80 °C for subsequent analysis. Meanwhile, a paralleled experiment was conducted on Wistar rats by oral gavage of 1.0 g/kg of AP based on our previous dosage experiment ($n = 20$). For the pharmacokinetic study of AP, serum samples in AP and Vac_AP groups were collected at different timepoints ($n = 4–8$).

### 2.3. Biochemical and liver histological analysis

Serum ALT, AST, liver and cellular GSSG/GSH were analyzed according to the instructions. Liver tissues were maintained in 10% neutral formalin, then embedded in paraffin and liver tissues were sliced at 5 μm for hematoxylin and eosin (H&E) staining. The degree of liver injury was scored according to Ref. [11].

### 2.4. Untargeted metabolomics analysis on serum sample with GC-MS

Serum samples stored at −80 °C were thawed and vortexed for 5 s at room temperature. A total of 30 μL of serum sample was added to tube containing 10 μL of internal standard (0.1 mg/mL dulcitol), and vortexed for 5 s. Then, 120 μL of ice-cold methanol/chloroform (3:1) was added, the resulting mixture was vortexed for 30 s and placed at −20 °C for 20 min before centrifugation at 16 000 g and 4 °C for 15 min. Quality control (QC) sample was prepared in parallel by pooling a small part of serum from each sample and analyzed with the same procedure. The supernatant was utilized for untargeted metabolomics analysis with GC-MS. The instrumental analysis and data preprocessing were described as our previous method [12].

### 2.5. Quantitation of AP and 2-HB with targeted metabolomics in serum and cecum samples

For serum samples, 5 μL of d3-2-HB (20 μg/mL, internal standard for 2-HB) and 5 μL of phenacetin (2 μg/mL, internal standard for AP) were added to 25 μL of serum sample, and 165 μL of methanol was added into each sample to precipitate protein. After votex for 1 min, the samples were centrifuged (14 000 rpm, 4 °C, 10 min) and the supernatant was transferred into tubes for further analysis. For 2-HB calibration curve, 25 μL of 2-HB standard solutions (125 ng/mL, 250 ng/mL, 500 ng/mL, 1 μg/mL, 2.5 μg/mL, 5 μg/mL, 10 μg/mL, 50 μg/mL, 100 μg/mL, and 200 μg/mL) were mixed with 5 μL of d3-2-HB (20 μg/mL) and 170 μL of methanol and prepared with the same method. For AP calibration curve, 2.5 μL of AP standard solutions (10 ng/mL, 20 ng/mL, 100 ng/mL, 500 ng/mL, 1 μg/mL, 2 μg/mL, 5 μg/mL, 10 μg/mL, 20 μg/mL, 50 μg/mL, 100 μg/mL, 200 μg/mL, and 500 μg/mL) were mixed with 22.5 μL of blank serum, 5 μL of phenacetin (2 μg/mL) and 170 μL of methanol and prepared with the same method.

A total of 50 mg cecum content of each mouse was weighed and added with 400 μL of water. The samples were grinded thoroughly and centrifuged (14 000 rpm, 4 °C, 10 min). 100 μL of supernatant was transferred into the tube and 295 μL of methanol and 5 μL of d3-2-HB (20 μg/mL) were added, after votex for 1 min, the samples were centrifuged (14 000 rpm, 4 °C, 10 min). The supernatant was transferred into a new tube and concentrated to dry under nitrogen. The dried sample was dissolved in 100 μL of methanol, after votex for 2 min and centrifuged at 14 000 rpm for 2 min, the supernatant was transferred into tubes for further analysis. For calibration curve of 2-HB, 100 μL of standard solution (31.25, 62.5, 125, 250, 500, and 1000 ng/mL) was mixed with 5 μL of d3-2-HB (20 μg/mL) and 295 μL methanol and prepared with the same method.

The quantitation of AP and 2-HB was analyzed with LC20AD (Shimadzu) coupled with AB Sciex Triple Quadrupole 4500. AP and 2-HB were separated through a C18 column (5 μm, 2 mm × 25 mm). The mobile phase was water with 0.1% formic acid (mobile phase A) and acetonitrile (mobile phase B). At a flow rate of 0.25 mL/min, a gradient was used as follows: 0–1.0 min,3% B; 1.0–1.1 min, 3% B to 50% B; 1.1–2 min, 50% B; 2.0–2.1 min, 50% B to 3% B; 2.1–2.9 min, 3% B. The column was maintained at 40 °C, and the samples were kept at 4 °C in an auto sampler during the entire analysis. The response of AP and phenacetin was measured in positive mode ($[M+H]^+$). The Q1 Mass (Da)/Q3 Mass (Da) for AP and phenacetin was 152.0/110.1 and 180.1/110.0, respectively. The response of 2-HB and d3-2-HB was measured in negative mode ($[M-H]^-$). The Q1 Mass (Da)/Q3 Mass (Da) for 2-HB and d3-2-HB was 103.0/57.1 and

106.0/59.1, respectively. Data were acquired and processed with Analyst 1.5.2 system software (AB SCIEX™, Foster City, CA, USA).

### 2.6. Gut microbiota analysis with 16S rRNA gene sequencing

Gut bacterial DNA extraction and 16S rRNA gene sequencing were conducted according to the method previously published [12]. Briefly, bacterial DNA of cecum contents was extracted with bacteria DNA stool mini kit following the manufacturer's instructions. The extracted DNA samples were used as template for amplification of the V3 region of 16S rRNA gene. The PCR amplification, pyrosequencing of PCR amplicons and quality control were performed on Ion PGM™ System according to Ref. [13]. Raw fastq data was quality-filtered for further analysis. Operational taxonomic units (OTUs) were delineated at 97% similarity level with Mothur software. Raw fastq files were subsequently deposited to the Sequence Read Archive database under the accession number PRJNA546452.

### 2.7. Preparation of primary hepatocytes from mice

Mouse primary hepatocytes were isolated by two-step collagenase perfusion protocol [14]. Briefly, mice were anesthetized with 1% pentobarbital sodium solution by intraperitoneal injection. Then, the mouse liver was perfused with perfusion medium I via portal vein for 10 min. Next, the liver was perfused with medium containing collagenase type I for 10 min. After adequate digestion, the liver was dissected in sterile dish and passed through a 100 μm filter followed by centrifugation for 2 min at 600 rpm. The supernatant was discarded and hepatocytes pellet was resuspended in DMEM medium. The above washing step was repeated for three times. Then the hepatocytes were purified with percoll regent and then seeded on plates with 10% FBS DMEM for further experiments.

### 2.8. Cell viability test under the treatment of 2-HB

Cells were seeded on a 96 well plate with a proper density. After 24 h, cells were incubated with or without 2-HB (5–40 mM) for 24 h or 48 h. Cell viability was measured with CCK-8 kit, with the addition of CCK-8 regent (10%) into the medium following the incubation at 37 °C for 1 h. The absorbance was measured at 450 nm (the main wavelength) and 600 nm (the secondary wavelength) and the viability was calculated as the percentage of control.

### 2.9. The protective effects of 2-HB on AP-induced cell injury

First, the IC50 of AP in BRL3A, AML12 and mouse primary hepatocytes were evaluated. Different concentrations of AP (3.125, 6.25, 12.5, 25, and 50 mM) were incubated with cells for 24 h or 48 h. The cell viability was analyzed with CCK-8 kit. And these cell lines were separately treated with AP at its IC50 dosage and different concentrations of 2-HB. BRL3A cells were treated with 9 mM of AP and 2-HB (5, 10, 20, and 40 mM) for 48 h. AML12 cells were treated with 14 mM of AP and 2-HB (5, 10, 20, and 40 mM) for 48 h. Mice primary liver cells were treated with 17 mM of AP and 2-HB (5, 10, 20, and 40 mM) for 24 h. Cell viability was measured with CCK-8 kit and calculated as the percentage of control group.

### 2.10. Functional investigation of 2-HB in AP-induced acute liver injury in mice

To study the impact of 2-HB on AP-induced liver injury, male C57 mice were divided into four groups as follows: Con group ($n = 5$), 2-HB group ($n = 6$), AP group ($n = 7$) and 2-HB + AP group ($n = 7$). 2-HB (250 mg/kg) were intraperitoneally injected into C57 mice in 2-HB and 2-HB + AP groups for 4 days, and 30 min after the last injection, 400 mg/kg of AP was orally administered to mice in AP and 2-HB + AP groups. After 24 h, all mice were anesthetized with 2% pentobarbital sodium and samples were collected and stored at −80 °C for subsequent analysis. For the pharmacokinetic study of AP, serum samples in AP and 2-HB + AP groups were collected at the time points of 0, 10 min, 0.5 h, 1 h, 3 h, 8 h, and 24 h. Three mice in AP or 2-HB + AP group at each time point were used in this study and each serum sample was analyzed twice with instrument ($n = 6$).

### 2.11. β-GD activity assay in cecum content

A total of 100 mg of cecum contents from each rat of Con, Vac, AP and Vac_AP groups was homogenized with 100 μL of lysis buffer and grinded with magnetic beads for 1 min. After centrifuged at 8000 g for 10 min (4 °C), the supernatant was transferred to another clean tube for further analysis. Total protein concentration of each sample was assayed and the samples were adjusted to the same protein concentration before β-glucuronidase (β-GD) assay. The assay was performed based on articles previously published [15]. Briefly. P-nitrophenyl-b-D-glucuronide acid (PNPG) was used as the probe substrate of β-GD. The incubation mixture with a total volume of 0.1 mL consisted of 48 μL of 0.2 M phosphate buffer (pH 6.8), 50 μL of sample and 2 μL of PNPG (200 mM, final concentration). PNPG hydrolysis was performed at 37 °C for 30 min. The signal of the hydrolytic metabolite of PNPG (PNP) was detected at 405 nm every 1 min, by a Synergy H1 Hybrid Multi-Mode Microplate Reader (BioTek, USA). The reaction rate was calculated based on the $OD_{405}$ and used for the comparison of β-GD activity between groups.

### 2.12. Real-time RT-PCR analysis on gene expression

Total RNA of liver tissue was extracted using TRIzol reagent (Invitrogen, Carlsbad, CA) and quantified by UV absorption (Colibri, Titertek Berthold). Following quantification, reverse transcript reaction was performed with a reverse transcript enzyme (Life technologies, Invitrogen) according to the manufacturer's instructions. Quantitative amplification by PCR was carried out using SYBR Green Master Mix regent by Biorad CFX Connect system. Cycle numbers of both 18s (as an internal control) and cDNAs of interest were used to calculated relative expression levels of the genes of interest.

### 2.13. Western blot

Liver protein was extracted with a commercial lysis buffer (Shanghai beyotime Biotechnology Company) added with 1% of phosphatase inhibitor cocktail 2 and phosphatase inhibitor cocktail 3 (Sigma) according to well-established protocols. The concentration of total protein was determined with Pierce™ BCA protein assay kit (Thermo Scientific). Then the samples were adjusted to the same concentration and mixed with loading buffer, and heated at 100 °C for 10 min. A total of 40 μg protein was loaded into each lane and separated by 10% SDS-PAGE gel, and then transferred to a PVDF membrane (Millipore). The membranes were blocked with 10% milk at room temperature for 90 min and then washed with TBST (20 mM Tris-HCl, 137 mM NaCl, and 0.1% Tween20, pH7.5) for three times at 10 min interval, following the incubation with primary antibodies for NQO-1 (Abcam), CYP2E1 (Abcam) and CYP3A4 (Abcam) overnight at 4 °C. The membranes were washed with TBST for three times, and incubated with the HRP-conjugated secondary antibodies for 2 h at room temperature. The membranes were exposed with SuperSignal West Pico Chemiluminescent Substrate

(Thermo Fisher Scientific, USA) and the bands were quantified with Amersham Imager 600 system (General Electric Company, USA).

### 2.14. Liver CYP450 enzymatic activity assay

S9 fractions were prepared from the liver to determine the activities of CYP2E1 and CYP1A2 according to previous method with some modifications [16]. Briefly, 250 mg of liver tissue in each group ($n$ = 5–10) was mixed with 1 mL of 100 mM potassium phosphate containing 0.15 M potassium chloride (pH = 7.4) and grinded with magnetic beads for 1 min. After centrifuged at 9000 g for 20 min, the supernatant was transferred to another clean tube and tested for the total protein concentration with BCA method. Each assay contained 99 μL of 0.1 M potassium phosphate buffer (pH 7.4), a NADPH-generating system (containing 0.1 M glucose 6-phosphate, 10 mM NADP+, and 10 IU/mL glucose-6-phosphate dehydrogenase, 40 mM $MgCl_2$), 20 μL of S9 fraction and 1 μL of probe substrate. Following a 3 min preincubation period in the absence of probe substrate, the reaction mixture was incubated for 30 min at 37 °C, and the reaction was stopped by adding 100 μL acetonitrile. LC20AD (Shimadzu) coupled with AB Sciex Triple Quadrupole 4500 system was utilized to measure the metabolites of CYP2E1 (6-hydroxy-chlorzoxazone) and CYP1A2 (acetaminophen).

### 2.15. PICRUSt analysis with 16S rRNA gene sequencing data

Phylogenetic Investigation of Communities by Reconstruction of Unobserved States (PICRUSt) analysis was performed with 16S rRNA gene sequencing data [17]. This method predicts the gene family abundance from the phylogenetic information with an estimated accuracy of 0.8. The OTU table was used as the input for metagenome imputation and was first rarefied to an even sequencing depth prior to the PICRUSt analysis. Next, the resulting OTU table was normalized by 16S rRNA gene copy number. The gene content was predicted for each individual. Then the predicted functional composition profiles were collapsed into level 3 of KEGG (Kyoto Encyclopedia of Genes and Genomes) database pathways.

### 2.16. Statistical analysis

Data are shown as means ± SEM unless otherwise noted. Statistical significance was determined with the unpaired two-tailed Student's $t$-test. The statistical significance of hepatic steatosis scores was evaluated with non-parametric Kruskal-Wallis test followed by the MannWhitney $U$ test. $p < 0.05$ was considered statistically significant.

## 3. Results

### 3.1. Vac pretreatment attenuates AP-induced acute liver injury in rats

First of all, to confirm the impact of gut microbiota on AP-induced liver injury, male SD rats were administered with single-dose of AP either orally (2.0 g/kg) or through intraperitoneal injection (1.0 g/kg). We found that serum ALT and AST levels were significantly elevated in both oral administration and intraperitoneal injection groups compared to control group. However, dramatic inter-individual variation in serum ALT and AST was only present in orally administrated rats (Fig. 1A), but not those under intraperitoneal injection (Fig. 1B). Given the fact that the absorption process of intraperitoneal injection is absent of impact from gut microbiota, high inter-individual variation of AP-induced liver injury in orally administrated rats was probably due to gut microbial influence on AP pharmacokinetics. Then, the microbial impact on AP-induced liver injury was investigated in male SD rats pretreated with or without Vac for 4 consecutive days prior to a single-dose AP (2.0 g/kg) administration. After 24 h of AP treatment, we found that pretreatment of Vac significantly attenuated serum ALT and AST elevation compared to that of AP alone (Fig. 1C), which was proved by liver histological analysis (Fig. 1D). Meanwhile, a paralleled experiment was conducted in Wistar rats, which showed consistent results with those observed in SD rats (Figs. S1A and B). These results indicated that Vac pretreatment could attenuate AP-induced acute liver injury in rats.

### 3.2. Vac pretreatment decreases the bioavailability of AP and ratio of GSSG/GSH

To investigate whether the attenuation of AP-induced liver injury by Vac pretreatment was associated with changes of AP bioavailability, pharmacokinetics of AP were compared between AP and Vac_AP groups either in SD or Wistar rats. The results showed that serum concentrations of AP at the 2nd, 4th, 8th, 24th h and $AUC_{0\text{-}t}$ were significantly lower in Vac_AP group than in AP group in either SD or Wistar rats (Fig. 2A, Fig. S1C). Since the serum concentration of AP is partially dependent on the extent of AP reabsorption in intestinal tract through deglucuronidation of conjugated AP by bacteria-derived β-GD [18,19], we therefore expected whether Vac pretreatment altered the activity of β-GD or not. The activity of β-GD was measured in cecum contents. The results showed that the activity of β-GD was significantly inhibited by Vac pretreatment (Fig. 2B), suggesting that the reduced serum concentration of AP in Vac-pretreated rats was probably associated with the inhibition of bacterial β-GD activity.

Since the AP-induced liver injury is partly due to depletion of GSH [5], the ratio of GSSG/GSH was compared between AP and Vac_AP groups. We found that the ratio of GSSG/GSH was dramatically reduced in Vac_AP rats compared to AP rats (Fig. 2C), suggesting that Vac pretreatment increased levels of GSH, rather than its oxidative product GSSG. In line with the increased levels of GSH, Vac pretreatment resulted in up-regulated mRNA expression of *Nqo-1* and *Gclc* gene, and down-regulated *Tnf-α* and *Il-1β* (Fig. 2D).

In addition, the protein expression of CYP2E1 and CYP3A4, and enzyme activity of CYP2E1 and CYP1A2 were measured in liver tissue, which regulate the formation of toxic NAPQI from AP [20,21]. There were no significant differences in CYP3A4 protein expression and CYP1A2 activity between the two groups (Figs. 2E and F, Fig. S2), except for the up-regulated protein expression and activity of CYP2E1 in Vac_AP group (Figs. 2G and H, Fig. S2). Collectively, these results suggested that the protection of Vac pretreatment against AP-induced liver injury may not be due to the reduction of NAPQI product, but associated with decreased bioavailability of AP and increased ratio of GSH/GSSG.

### 3.3. Vac pretreatment elevates 2-HB in both cecum and serum

In addition to the pharmacokinetics change, previous study indicates that endogenous metabolite derived from gut microbiota may also contribute to AP-induced hepatotoxicity [9]. We therefore investigated the mechanism underlying the protective effect of Vac pretreatment against AP-induced liver injury using GC-MS-based untargeted metabolomics on serum samples. First of all, we observed that Vac treatment not only significantly altered the metabolic profile at baseline, but also in AP treated-rats (Fig. 3A), suggesting that Vac treatment could on the one hand alter the metabolism of host, on the other hand, reverse the endogenous metabolism in AP-treated rats. Then, differential metabolites

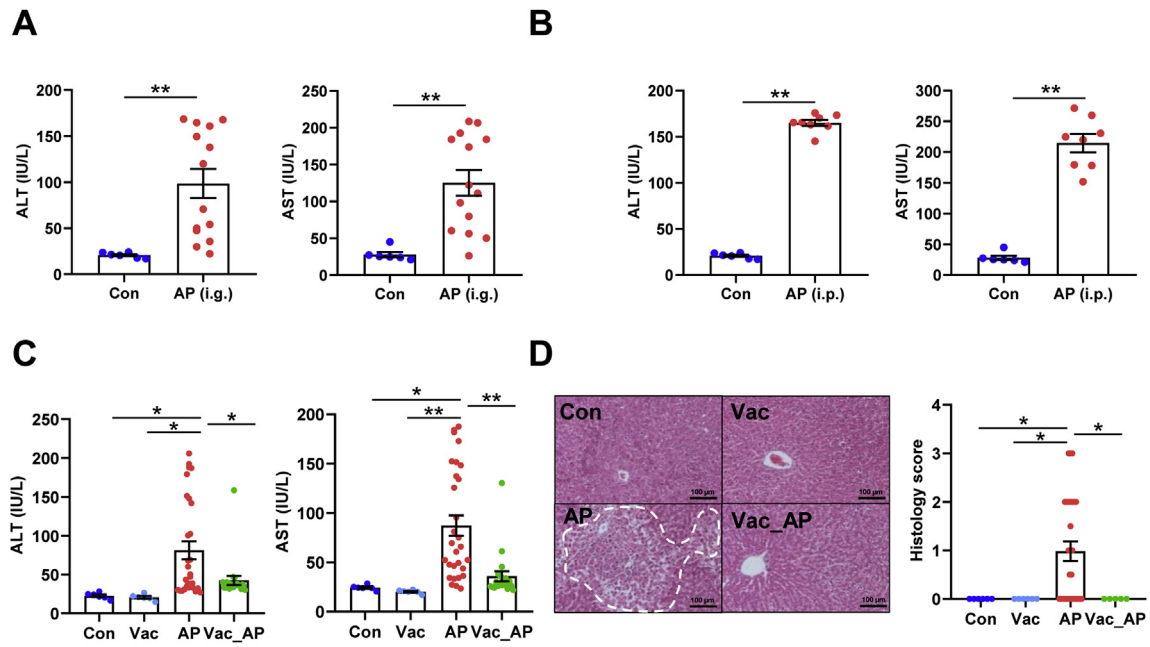


**Fig. 1.** Vac pretreatment attenuates AP-induced acute liver injury in rats. (A and B) Serum ALT and AST levels. i. g and i. p represent oral gavage or intraperitoneal injection with a single dose of 2.0 g/kg or 1.0 g/kg of AP, respectively ($n = 6–14$). (C and D) Serum ALT, AST, hepatic H&E staining, and histology score in SD rats treated with Vac (100 mg/kg, twice a day) and/or with AP (i.g, 2.0 g/kg). $n = 5–6$ in Con or Vac group. $n = 29$ in AP and 20 in Vac_AP groups. Data were mean ± S.E.M. The magnification of H&E staining photograph is 200×. $^{*}P < 0.05$; $^{**}P < 0.01$.

among groups were determined with the double criteria of VIP>1.0 in OPLS-DA model and $p < 0.05$ in Student's *t*-test, in which a total of 13 differential metabolites were identified and visualized with a heatmap (Fig. 3B). These 13 differential metabolites were further uploaded to MetaboAnalyst (https://www.metaboanalyst.ca/) for pathway enrichment analysis, and 9 pathways were enriched with criteria of $p < 0.05$ including pathways involved in propanoate metabolism, amino acids metabolism (i.e. phenylalanine and tyrosine, beta-alanine, asparate, alanine, cysteine, malate-asparate shuttle and glucose-alanine cycle) and urea cycle (Fig. 3C). Propanoate metabolism pathway was the most significant pathway with the lowest *p* value, which included 2-HB, beta-alanine, 2-ketoglutaric acid and glutamic acid. All these four metabolites were increased by AP treatment compared to Con group, whereas 2-HB was one of the most significantly altered metabolites (Table S1). Furthermore, we quantified the concentrations of 2-HB in both cecum content and serum with or without AP treatment by using targeted metabolomics based on LC-MS/MS. The results showed that Vac pretreatment significantly elevated 2-HB levels in cecum content with or without AP treatment (Fig. 3D), suggesting gut-derived 2-HB was stimulated in Vac. Consistent with this finding, Vac pretreatment also increased levels of 2-HB in serum before AP treatment (Fig. 3E). However, serum 2-HB level was lower in Vac_AP group than AP group 24 h after AP treatment, which was in line with the untargeted metabolomics result (Fig. 3E).

To test whether the increased concentration of 2-HB by Vac treatment was due to altered gut microbiome, we compared the gut microbiota profiles by using 16S rRNA sequencing between AP and Vac_AP groups. The PCoA showed that AP and Vac_AP groups were clearly separated (Fig. 3F). At the phylum level, the relative abundance of Firmicutes and Bacteroides were dramatically decreased, while the abundance of Proteobacteria and Fusobacteria were greatly enriched in Vac_AP group (Fig. 3G). Then, a total of 50 genera with relatively higher abundance was chosen and compared between AP and Vac_AP groups, in which the relative abundance of 9 g-negative and 16 g-positive bacteria genera were either significantly increased or decreased by Vac pretreatment (Fig. S3). Functional annotation of gut bacteria showed that propanoate metabolism pathway was significantly enriched in Vac_AP group than AP group (Fig. 3H), which is consistent with the observation of serum metabolomics (Fig. 3C). In addition, since 2-HB is generated from 2-oxobutanoate by lactate dehydrogenase (LDH) (from Kyoto Encyclopedia of Genes and Genomes database, https://www.kegg.jp/), which is also present in some kinds of gut microbiota [22–25], we specially analyzed the abundance of LDH-expressing bacteria. Interestingly, we observed that the relative abundance of LDH-expressing bacteria was also increased in Vac_AP group (Fig. 3I). Alltogether, our results suggest that increased 2-HB by Vac treatment may be due to altered gut microbiota.

### 3.4. 2-HB attenuates AP-induced cellular toxicity

To investigate the biological function of 2-HB, different hepatocytes were treated with 2-HB at a series of concentrations including rat-derived liver cell line BRL3A, mice-derived liver cell line AML12 and mice primary hepatocytes. Interestingly, 2-HB treatment enhanced cell viability to different extent in AML-12 and mice primary hepatocytes, but not BRL3A (Figs. S4A–C). We then asked whether 2-HB could influence AP-induced cell toxicity. The IC50 of AP on these three cell lines were determined first (Figs. S4D–F), which were used for subsequent experiments with or without addition of 2-HB for 24 or 48 h. We found that addition of 2-HB significantly attenuated the AP-induced cell toxicity regardless of species difference in cell origin (Figs. 4A–C). Representative photographs of BRL3A cells treated with AP for 48 h in the presence or absence of 2-HB co-culture are presented in Fig. 4D. In line with the cell viability results, AP treatment resulted in a large portion of dead and floating cells, which was obviously improved by 2-HB (Fig. 4D). Furthermore, we observed that 2-HB addition decreased the ratio of GSSG/GSH in mice primary hepatocytes compared to AP alone (Fig. 4E). Our current results indicated that 2-

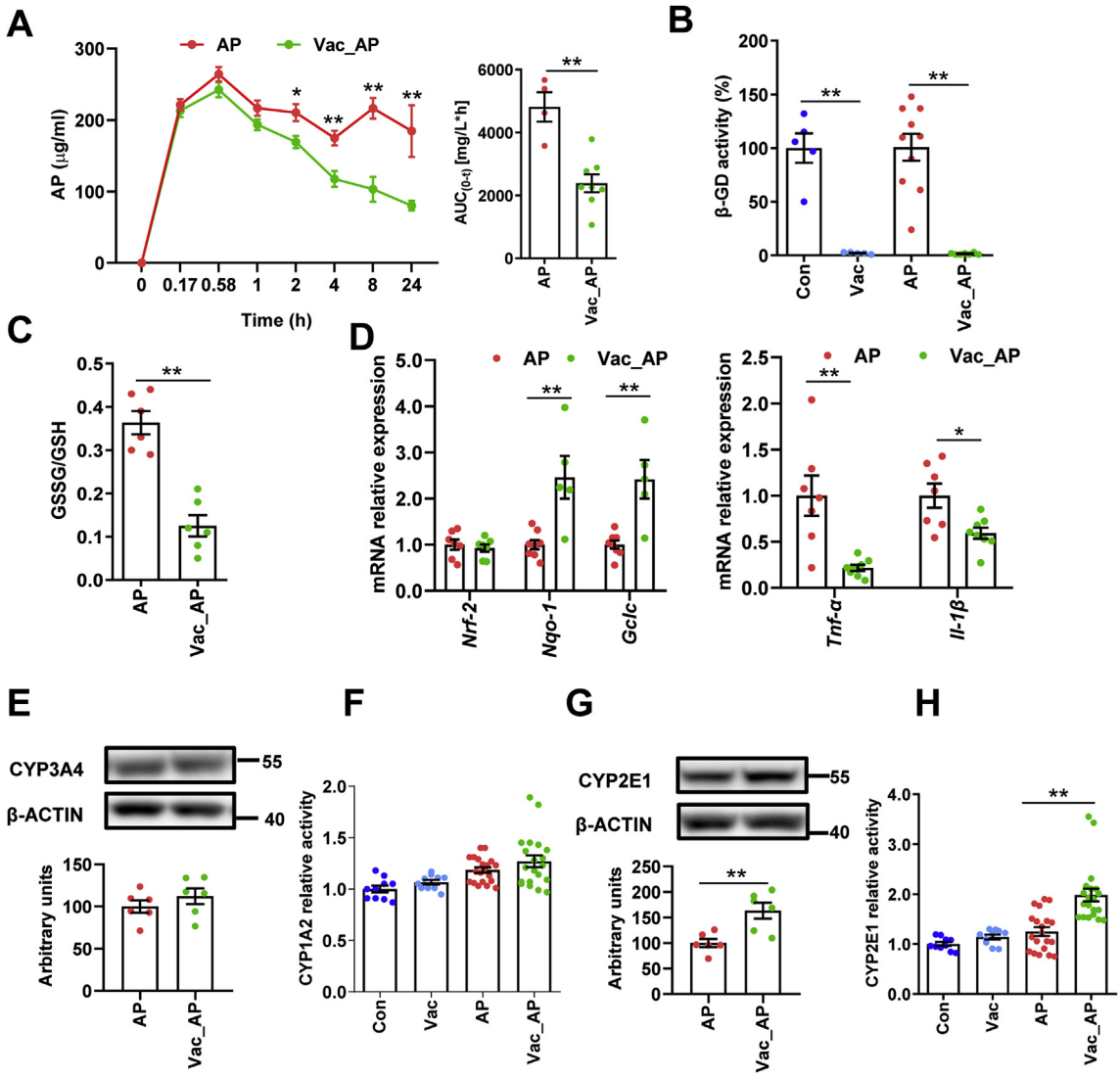


**Fig. 2.** Vac pretreatment decreases the bioavailability of AP and ratio of GSSG/GSH. (A) The serum concentrations of AP in SD rats at different time points ($n = 4$). (B) The activity of β-glucuronidase (β-GD) in cecum. $n = 5$ in Con or Vac group, and 10 in AP or Vac_AP group. (C and D) Hepatic GSSG/GSH and mRNA expression of genes ($n = 6$–8). (E and G) The hepatic protein levels of CYP3A4 and CYP2E1 ($n = 6$) as well as (F and H) enzymic activity of CYP1A2 and CYP2E1 measured with LC-MS/MS ($n = 10$ in Con or Vac group and 20 in AP or Vac_AP group). Data were mean ± S.E.M. $^{*}P < 0.05$, $^{**}P < 0.01$.

HB protected AP-induced cell toxicity in either rat- or mouse-derived cell lines.

### 3.5. 2-HB treatment protects AP-induced acute liver injury in mice

Given the observed evidence, we hypothesized that the attenuation on AP-induced liver injury by Vac pretreatment was probably due to 2-HB production. We observed the impact of 2-HB on AP-induced liver injury in a group of male C57 mice, which were orally given with single-dose of AP (400 mg/kg) following 3 days of 2-HB (250 mg/kg per day, i. p) treatment. Results showed that AP treatment induced significant liver injury in mice, whereas 2-HB pretreatment effectively protected mice from severe liver injury (Figs. 5A and B). Moreover, we found that 2-HB decreased the peak concentration of serum AP and reduced $AUC_{0\text{-}t}$ (Fig. 5C). In addition, the serum concentration of 2-HB was also detected before and after AP administration. We observed that intraperitoneally injection of 2-HB definitely increased serum levels of 2-HB, especially within the 1st h after AP treatment (Fig. 5D). Moreover, 2-HB pretreatment also inhibited mRNA expression of genes involved in mediating inflammation (*Tnf-α*, *Il-1β*) (Fig. 6A), cell proliferation process (*Btg2*, *Ccng1*) and DNA damage induced genes (*Ddit4l*, *Gadd45α*) (Fig. 6C) that were stimulated by AP treatment, as well as the regulation of genes in anti-oxidative pathways such as *Nqo-1*, *Txnrd1*, *Car3* (Fig. 6B) and down-regulation of genes related to hepatotoxicity (*Krt8*, *Krt18*) (Fig. 6C). In addition, 2-HB did not alter the protein expression of hepatic CYP2E1 or NQO-1 in AP-treated mice (Fig. 6D, Fig. S5). Overall, these data highlighted that 2-HB was protective against AP-induced liver injury in mice.

## 4. Discussion

In our current study, we demonstrated that Vac pretreatment attenuated AP-induced liver injury in rats, and altered the composition of gut microbiota. Then, our untargeted metabolomics revealed the significant metabolic change by Vac pretreatment. Moreover, we found 2-HB was elevated in serum by Vac pretreatment, which could reduce AP-induced toxicity in either rat- or

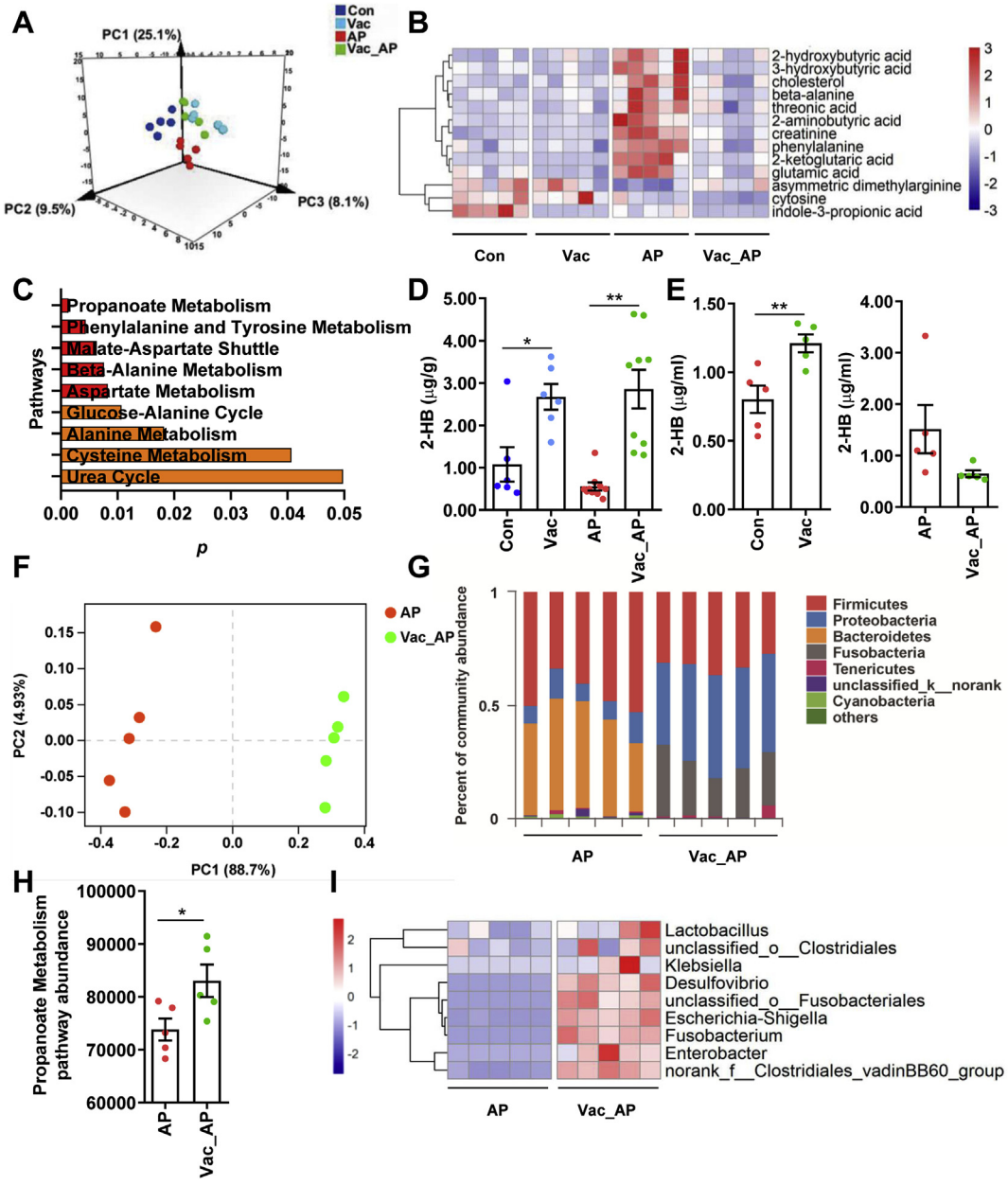


**Fig. 3.** Vac pretreatment elevates 2-HB in both cecum and serum. (A) PLS-DA plot of serum metabolites ($n = 5$). (B) Differential metabolites among groups ($n = 5$). (C) Pathway analysis based on the 13 differential metabolites in B. The quantitation of 2-HB in cecum contents (D) and serum (E) of rats 24 h after AP gavage ($n = 5–8$). (F–G) PCoA analysis at OTU level and column diagram at phylum level based on 16S rRNA gene sequencing ($n = 5$). (H) The abundance of propanoate metabolism pathway based on PICRUSt analysis of 16S rRNA gene sequencing ($n = 5$). (I) Heatmap of the relative abundance of LDH-producing bacteria at genus level ($n = 5$). Data were mean ± S.E.M. $^{*}P < 0.05$; $^{**}P < 0.01$.

mouse-derived cell lines or primary hepatocytes, as well as acute liver injury in mice.

AP-induced liver injury has been extensively investigated so far; however, the underlying mechanism is not fully elucidated. In addition to the conventional theory of NAPQI production [3,5], emerging evidence has indicated that the extent of AP-induced liver injury is dependent on microbial composition because of the extensive co-metabolism on xenobiotic between gut microbiota and host [7,8]. Previously, Nicholson group demonstrated that the character of basal metabolic profile is predictive for the extent of AP-induced liver injury [11], in which microbial metabolites such as taurine are involved. Moreover, the variation of urine p-cresol in human subjects influences the metabolism of AP [7]. Recently, the impact of gut microbiota on AP-induced liver injury is associated with changes of GSH levels [9] or alteration of AP metabolism [8,11]. In our current study, we were the first to observe that obvious inter-individual variation in levels of serum ALT and AST existed in AP orally treated rats, but not in those with intraperitoneal injection. It is reasonable that the bioavailability of orally administrated xenobiotics is apt to be impacted by more factors than intraperitoneal injection, in particular gut microbiota [6]. We further found that Vac pretreatment decreased the levels of serum ALT and AST and the extent of liver necrosis caused by AP in either SD or Wistar rats. Vac is a potent antibiotic against gram-positive bacteria and with limited systemic impacts due to non-absorptive character in intestine [10,26,27]. As a result, Vac is frequently used for investigating the role of gut microbiota in various studies [28–30]. Our results have proved that alteration of gut microbiota is a critical

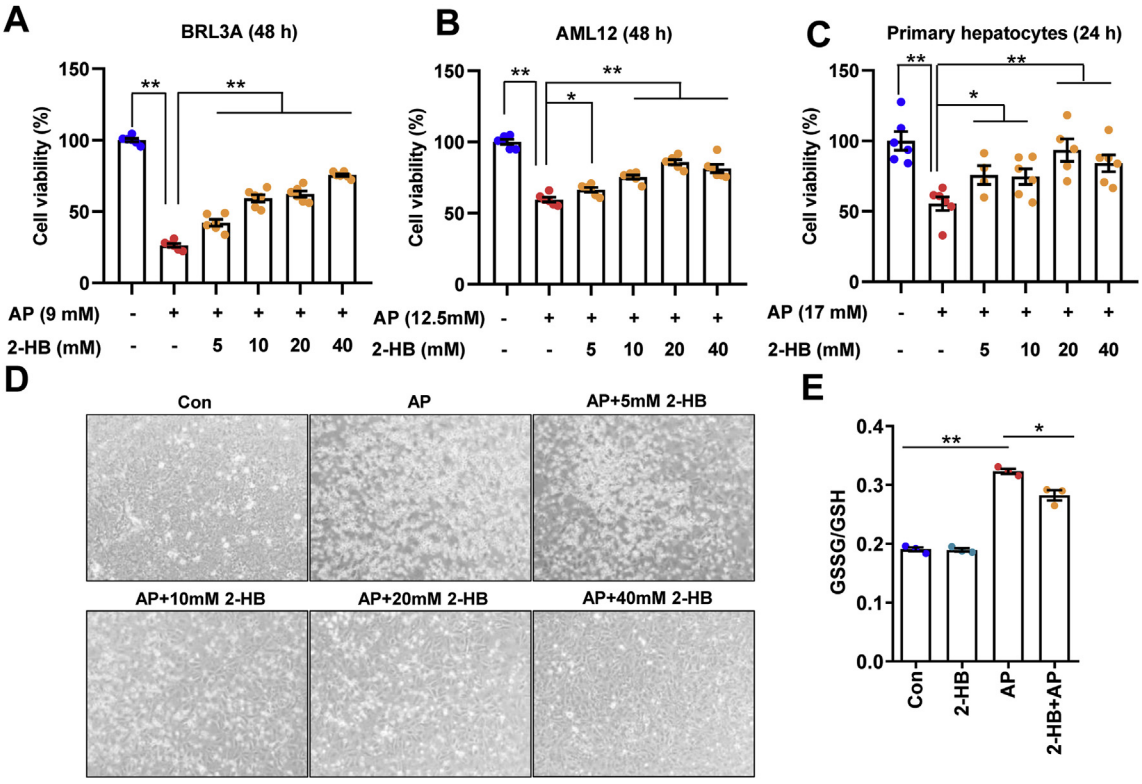


**Fig. 4.** 2-HB attenuates AP-induced cellular toxicity. (A) BRL3A cells, (B) AML12 cells, and (C) mouse primary hepatocytes were treated with AP alone or in combination with 5–40 mM 2-HB for indicated periods, and cell viability was measured with CCK-8 kit ($n = 6$). (D) Representative photographs of BRL3A cells treated with AP alone or in combination with 5–40 mM 2-HB for 48 h (The magnification of photographs is 100×). (E) Cellular GSSG/GSH was analyzed in primary hepatocytes treated with AP alone or in combination of 5 mM 2-HB for 24 h ($n = 3$). Data were mean ± S.E.M. $^{*}P < 0.05$, $^{**}P < 0.01$.

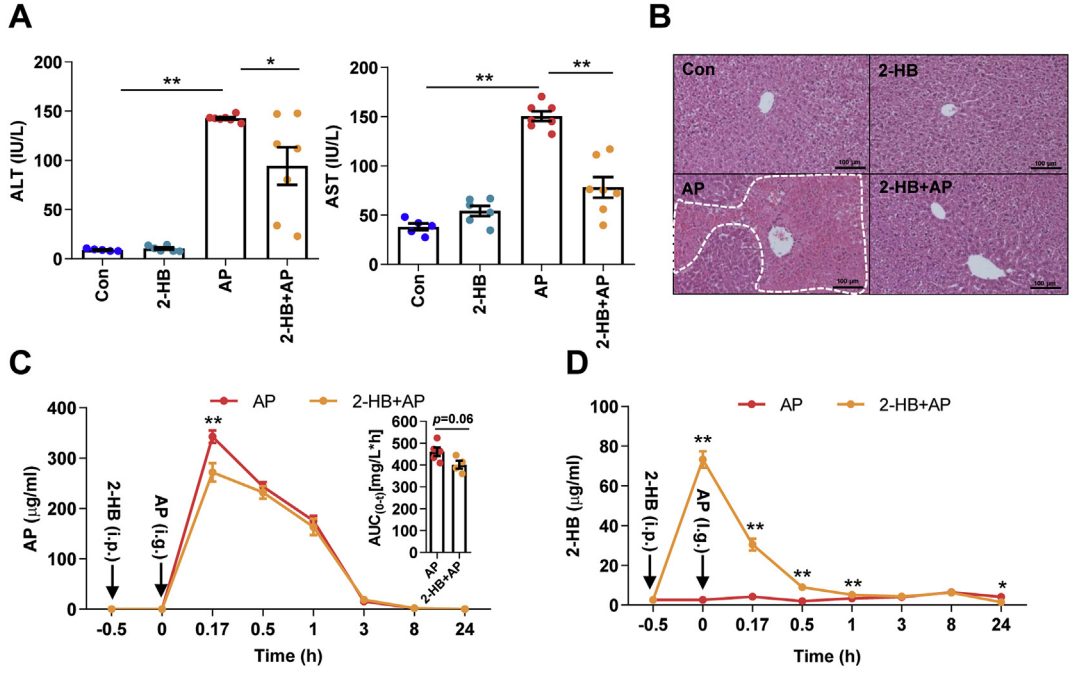


**Fig. 5.** 2-HB treatment protects AP-induced acute liver injury in mice. Mice were intraperitoneally injected with 2-HB (250 mg/kg, once a day) for 4 days and administered with a single dose of AP (400 mg/kg) 30 min after the last injection of 2-HB. (A–B) Serum ALT, AST, and liver histology in mice 24 h after AP treatment ($n = 5–7$). $^{*}P < 0.05$, $^{**}P < 0.01$. (C–D) Serum concentrations of AP and 2-HB quantified with LC-MS/MS in mice treated with AP and/or 2-HB ($n = 6$). $^{*}P < 0.05$, $^{**}P < 0.01$ compared to the same time point between the two groups. Data were mean ± S.E.M.

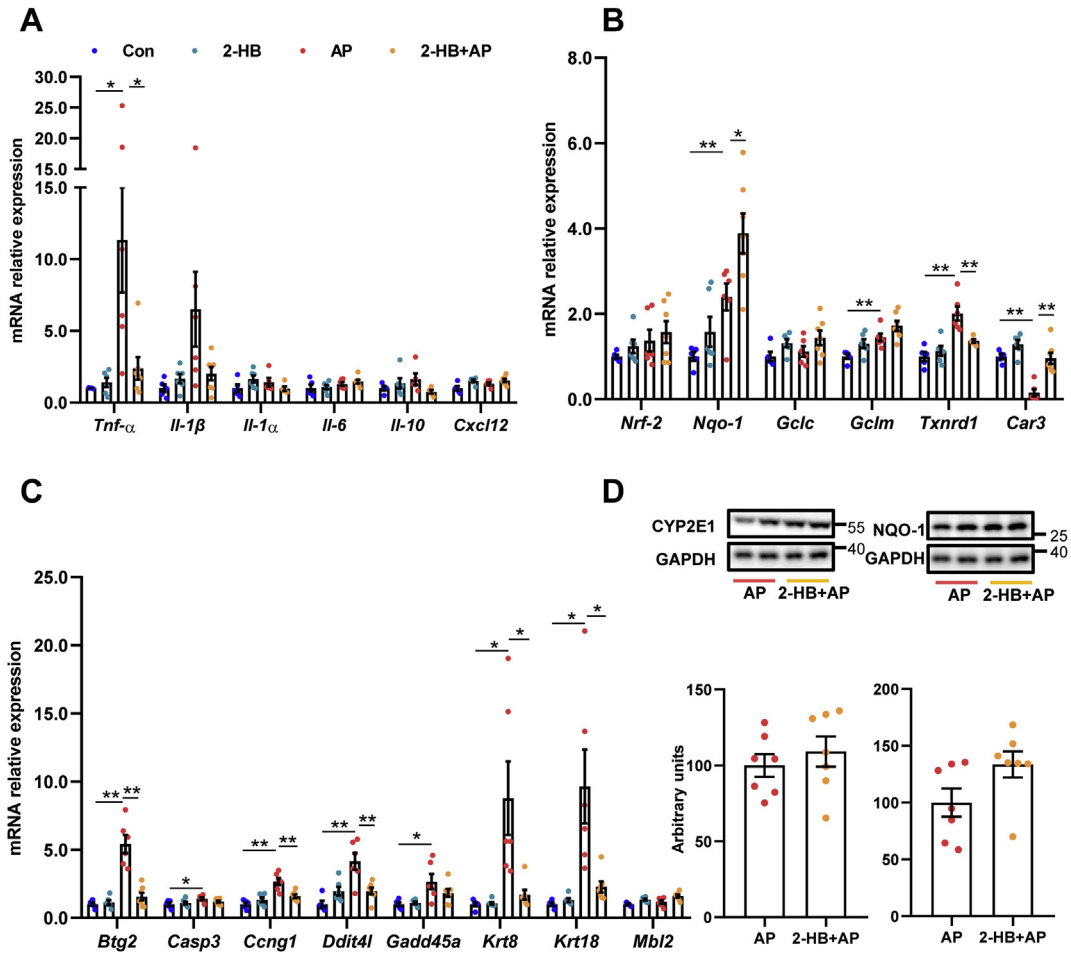


**Fig. 6.** 2-HB normalizes gene expression. (A) Inflammation related genes. (B) Oxidative stress related genes. (C) Cell proliferation and DNA damage induced genes. (D) Hepatic CYP2E1 and NQO-1 protein levels. $n = 5–7$ in (A-D). Data were mean ± S.E.M. $^{*}P < 0.05$, $^{**}P < 0.01$.

factor in determining the extent of AP-induced liver injury. Moreover, we found that Vac pretreatment significantly decreased the bioavailability of AP. Since the bioavailability of AP is influenced by intestinal absorption of AP, which is deglucuronidated by microbiota produced β-GD [18,19], we showed that Vac pretreatment greatly depleted the activity of β-GD in cecum contents. Therefore, it is possible that the depletion of intestinal β-GD reduces the absorption of AP. Nevertheless, the change of AP bioavailability cannot fully explain the reduced hepatotoxicity by Vac pretreatment. Moreover, the expression of CYP2E1 protein was even up-regulated in Vac pretreated group, which indicates that the protective effect of Vac on AP-induced liver injury was not due to reduced NAPQI production.

Metabolomics is increasingly applied to investigate the underlying mechanisms of drug activity/toxicity because metabolomics is a unique approach for quantitatively measurement of the time-related metabolic response of living systems to pathophysiological stimuli or genetic modification simultaneously [31,32]. Gong et al. [9] reveals that gut microbiota determine the diurnal variation of AP-induced liver injury through microbial metabolite, 1-phenyl-1,2-propanedione by using untargeted metabolomics. In our current study, an untargeted GC-MS-based metabolomics was adopted to test whether there are metabolites involved in attenuation of AP-induced liver injury by Vac pretreatment. Our results showed that the metabolic profile of AP was very different from others. Then, a total of 13 differential metabolites were identified between Con and AP groups that were restored by Vac pretreatment, suggesting that these metabolites were relevant to AP-induced hepatotoxicity. Moreover, propanoate metabolism was one of the most significantly altered metabolic pathways enriched with these differential metabolites, in which metabolite 2-HB attracted our attention because of its involvement in propanoate metabolism and dramatic fold change between Con and AP groups. Consistently, our targeted metabolomics analysis proved the elevation of 2-HB by Vac pretreatment in cecum content with or without AP treatment, suggesting that 2-HB production was associated with gut microbiota. Our results showed serum 2-HB level was lower in Vac_AP group than in AP group after 24 h of AP treatment. Oxidative stress or detoxification of xenobiotics in the liver can dramatically increase the rate of hepatic glutathione synthesis. Under such metabolic stress conditions, homocysteine is diverted from the transmethylation pathway (which forms methionine) into the transsulfuration pathway (which forms cystathionine). Alpha-ketobutyrate is produced when cystathionine is cleaved into cysteine that is incorporated into glutathione, and 2-HB is formed via a reaction catalyzed by LDH from alpha-ketobutyrate (http://www.hmdb.ca/metabolites/HMDB0000008). So the elevation of serum 2-HB in AP group after 24 h of AP treatment may be a stress response because of the upregulation of hepatic glutathione synthesis.

Meanwhile, 16S rRNA gene sequencing data indicated that Vac treatment obviously altered the composition of gut microbiota.

PICRUSt is a computational approach which uses an extended ancestral-state reconstruction algorithm to predict which gene families are present and then combines gene families to estimate the composite metagenome, thus can predict the functional composition of a metagenome using a database of reference genomes [17]. Based on the PICRUSt analysis of 16S rRNA gene sequencing data, the abundance of propanoate metabolism pathway involved in 2-HB producing was upregulated in Vac_AP group. At genus level, Vac treatment also upregulated the relative abundance of some LDH expressing bacteria such as *Lactobacillus*, *Clostridium*, *Fusobacterium*, *Desulfovibrio* [22–25]. As a result, we speculated that the attenuation on AP-induced liver injury by Vac pretreatment might be associated with the increase of 2-HB.

In line with our hypothesis, our results showed that 2-HB significantly improved cell viability under AP treatment in cell lines from either rats or mouse such as rat-derived BRL3A cells, mouse-derived AML12 cells and mouse primary hepatocytes, suggesting that the hepatoprotective effect of 2-HB is trans-species. Cellular GSH is critical for the detoxification of AP through conjugation with the toxic product NAPQI of AP. The accumulated NAPQI will deplete cellular GSH, resulting in oxidative stress-induced liver injury [33,34]. We found 2-HB reduced the AP-induced upregulation of liver GSSG/GSH in mouse primary hepatocytes that is consistent with its protective effect against AP-induced cell toxicity. Given the higher inter-individual variation of AP-induced liver injury among rats and observed trans-species protection of 2-HB against AP-induced toxicity in cell lines, the biological function of 2-HB was further validated in AP-treated mice, instead of rats. We observed that 2-HB prevented AP-induced liver injury in mice. Interestingly, 2-HB also decreased the $C_{max}$ and $AUC_{0\text{-}t}$ of AP, as well as regulated the expression of genes involved in inflammation, oxidative stress, cell proliferation and DNA damage process. Nevertheless, we are not quite clear about the link between 2-HB and AP bioavailability based on our current results. Further investigation will be conducted for explaining their potential relationship.

In summary, our current study demonstrates that Vac pretreatment attenuates AP-induced liver injury, alters serum metabolic and gut microbiota profiles in rats. The identified metabolite 2-HB has trans-species protective effect against AP-induced cell toxicity in either rat- or mouse-derived cells, which is further validated in mice. The protective effect of 2-HB is associated with the reduction of AP bioavailability and increase of GSH levels. This study confirms the impacts of gut microbiota on AP-induced hepatotoxicity, and sheds light on the potential to prevent AP-induced hepatotoxicity by modulating gut microbiota with antibiotic or other approaches such as prebiotic or probiotic if specific functional bacteria were determined in the future.

## Declaration of competing interest

The authors declare that there are no conflicts of interest.

## Acknowledgments

This work was funded by the National Natural Science Foundation of China (No. 81873059 & 81673662), the National Key Research and Development Program of China (No. 2017YFC1700200), Shuguang Scholar (16SG36) at Shanghai Institutions of Higher Learning from Shanghai Municipal Education Commission.

## Appendix A. Supplementary data

Supplementary data to this article can be found online at https://doi.org/10.1016/j.jpha.2019.11.003.

## References

[1] G. Ostapowicz, R.J. Fontana, F.V. Schiodt, et al., Results of a prospective study of acute liver failure at 17 tertiary care centers in the United States, Ann. Intern. Med. 137 (2002) 947–954.
[2] W. Bernal, G. Auzinger, A. Dhawan, et al., Acute liver failure, Lancet 376 (2010) 190–201.
[3] L.F. Prescott, Kinetics and metabolism of paracetamol and phenacetin, Br. J. Clin. Pharmacol. 10 (Suppl 2) (1980) 291S–298S.
[4] C.K. Gelotte, J.F. Auiler, J.M. Lynch, et al., Disposition of acetaminophen at 4, 6, and 8 g/day for 3 days in healthy young adults, Clin. Pharmacol. Ther. 81 (2007) 840–848.
[5] J.R. Mitchell, D.J. Jollow, W.Z. Potter, et al., Acetaminophen-induced hepatic necrosis. IV. Protective role of glutathione, J. Pharmacol. Exp. Ther. 187 (1973) 211–217.
[6] H.J. Haiser, P.J. Turnbaugh, Developing a metagenomic view of xenobiotic metabolism, Pharmacol. Res. 69 (2013) 21–31.
[7] T.A. Clayton, D. Baker, J.C. Lindon, et al., Pharmacometabonomic identification of a significant host-microbiome metabolic interaction affecting human drug metabolism, Proc. Natl. Acad. Sci. U.S.A. 106 (2009) 14728–14733.
[8] S.H. Lee, J.H. An, H.J. Lee, et al., Evaluation of pharmacokinetic differences of acetaminophen in pseudo germ-free rats, Biopharm Drug Dispos. 33 (2012) 292–303.
[9] S. Gong, T. Lan, L. Zeng, et al., Gut microbiota mediates diurnal variation of acetaminophen induced acute liver injury in mice, J. Hepatol. 69 (2018) 51–59.
[10] I.K. Yap, J.V. Li, J. Saric, et al., Metabonomic and microbiological analysis of the dynamic effect of vancomycin-induced gut microbiota modification in the mouse, J. Proteome Res. 7 (2008) 3718–3728.
[11] T.A. Clayton, J.C. Lindon, O. Cloarec, et al., Pharmaco-metabonomic phenotyping and personalized drug treatment, Nature 440 (2006) 1073–1077.
[12] X. He, N. Zheng, J. He, et al., Gut microbiota modulation attenuated the hypolipidemic effect of simvastatin in high-fat/cholesterol-diet fed mice, J. Proteome Res. 16 (2017) 1900–1910.
[13] X. Zhang, Y. Zhao, M. Zhang, et al., Structural changes of gut microbiota during berberine-mediated prevention of obesity and insulin resistance in high-fat diet-fed rats, PLoS One 7 (2012), e42529.
[14] Q. Wang, L. Jiang, J. Wang, et al., Abrogation of hepatic ATP-citrate lyase protects against fatty liver and ameliorates hyperglycemia in leptin receptor-deficient mice, Hepatology 49 (2009) 1166–1175.
[15] Z.M. Weng, P. Wang, G.B. Ge, et al., Structure-activity relationships of flavonoids as natural inhibitors against E. coli beta-glucuronidase, Food Chem. Toxicol. 109 (2017) 975–983.
[16] J.H. Jo, S. Kim, T.W. Jeon, et al., Investigation of the regulatory effects of saccharin on cytochrome P450s in male ICR mice, Toxicol. Res. 33 (2017) 25–30.
[17] M.G. Langille, J. Zaneveld, J.G. Caporaso, et al., Predictive functional profiling of microbial communities using 16S rRNA marker gene sequences, Nat. Biotechnol. 31 (2013) 814–821.
[18] N. Watari, M. Iwai, N. Kaneniwa, Pharmacokinetic study of the fate of acetaminophen and its conjugates in rats, J. Pharmacokinet. Biopharm. 11 (1983) 245–272.
[19] C.P. Siegers, K. Rozman, C.D. Klaassen, Biliary excretion and enterohepatic circulation of paracetamol in the rat, Xenobiotica 13 (1983) 591–596.
[20] C.J. Patten, P.E. Thomas, R.L. Guy, et al., Cytochrome P450 enzymes involved in acetaminophen activation by rat and human liver microsomes and their kinetics, Chem. Res. Toxicol. 6 (1993) 511–518.
[21] K.E. Thummel, C.A. Lee, K.L. Kunze, et al., Oxidation of acetaminophen to N-acetyl-p-aminobenzoquinone imine by human CYP3A4, Biochem. Pharmacol. 45 (1993) 1563–1569.
[22] S. Chaillou, M.C. Champomier-Verges, M. Cornet, et al., The complete genome sequence of the meat-borne lactic acid bacterium Lactobacillus sakei 23K, Nat. Biotechnol. 23 (2005) 1527–1533.
[23] M. Monot, C. Boursaux-Eude, M. Thibonnier, et al., Reannotation of the genome sequence of Clostridium difficile strain 630, J. Med. Microbiol. 60 (2011) 1193–1199.
[24] V. Kapatral, I. Anderson, N. Ivanova, et al., Genome sequence and analysis of the oral bacterium Fusobacterium nucleatum strain ATCC 25586, J. Bacteriol. 184 (2002) 2005–2018.
[25] J.F. Heidelberg, R. Seshadri, S.A. Haveman, et al., The genome sequence of the anaerobic, sulfate-reducing bacterium Desulfovibrio vulgaris Hildenborough, Nat. Biotechnol. 22 (2004) 554–559.
[26] R.C. Moellering Jr., Vancomycin: a 50-year reassessment, Clin. Infect. Dis. 42 (Suppl 1) (2006) S3–S4.
[27] N.J. Pultz, U. Stiefel, C.J. Donskey, Effects of daptomycin, linezolid, and vancomycin on establishment of intestinal colonization with vancomycin-resistant enterococci and extended-spectrum-beta-lactamase-producing Klebsiella pneumoniae in mice, Antimicrob. Agents Chemother. 49 (2005) 3513–3516.
[28] A. Zarrinpar, A. Chaix, Z.Z. Xu, et al., Antibiotic-induced microbiome depletion alters metabolic homeostasis by affecting gut signaling and colonic metabolism, Nat. Commun. 9 (2018) 2872.
[29] I. Hwang, Y.J. Park, Y.R. Kim, et al., Alteration of gut microbiota by vancomycin and bacitracin improves insulin resistance via glucagon-like peptide 1 in diet-

induced obesity, FASEB J. 29 (2015) 2397–2411.
[30] S. Fujisaka, J. Avila-Pacheco, M. Soto, et al., Diet, genetics, and the gut microbiome drive dynamic changes in plasma metabolites, Cell Rep. 22 (2018) 3072–3086.
[31] J.K. Nicholson, J.C. Lindon, E. Holmes, 'Metabonomics': understanding the metabolic responses of living systems to pathophysiological stimuli via multivariate statistical analysis of biological NMR spectroscopic data, Xenobiotica 29 (1999) 1181–1189.
[32] J.K. Nicholson, J. Connelly, J.C. Lindon, et al., Metabonomics: a platform for studying drug toxicity and gene function, Nat. Rev. Drug Discov. 1 (2002) 153–161.
[33] H. Jaeschke, T.R. Knight, M.L. Bajt, The role of oxidant stress and reactive nitrogen species in acetaminophen hepatotoxicity, Toxicol. Lett. 144 (2003) 279–288.
[34] H. Jaeschke, M.R. Mcgill, A. Ramachandran, Oxidant stress, mitochondria, and cell death mechanisms in drug-induced liver injury: lessons learned from acetaminophen hepatotoxicity, Drug Metab. Rev. 44 (2012) 88–106.